# Analysis of Response Variation in Fast and Precise Micrometer Stroke Positioning

Yoshihiro MAEDA
Department of Electrical and
Mechanical Engineering
Nagoya Institute of Technology
Gokiso, Showa, Nagoya 4668555, JAPAN
Email: ymaeda@nitech.ac.jp

Makoto IWASAKI
Department of Electrical and
Mechanical Engineering
Nagoya Institute of Technology
Gokiso, Showa, Nagoya 4668555, JAPAN
Email: iwasaki@nitech.ac.jp

***Abstract*—This paper presents an analysis of response variation in the fast and precise micrometer stroke positioning of table drive systems with rolling friction. The rolling friction in the mechanism behaves as a nonlinear and dynamic elastic component with a hysteresis property in a micro displacement region, which may cause the response variation in a sequential micrometer stroke positioning motion. In this study, a mechanism of the variation is analytically examined by using a rolling friction model. And then, a rolling friction model-based simple feedforward friction compensation is adopted to improve the positioning performance. The rolling friction model-based analysis and friction compensation are verified by numerical simulations and experiments using a prototype of linear motor-driven table systems.**

## I. Introduction

Requirements for the fast-response and high-precision positioning control are getting more severe in varieties of high performance mechatronic systems in industry, in order to achieve advantages in productivity and/or quality of products [1]. In addition, since the fast and precise positioning technology leads to a reduction of energy consumption due to shortening a time for manufacturing, studies on the fast and precise control techniques should be significant from a viewpoint of environmental protection. In recent years, a demand of shorter stroke positioning motions, i.e., micrometer stroke, is increasing for miniaturization of processing objects, and an effective position control technique for the micrometer stroke motion is strongly required [2]. However, it is generally known that rolling friction in the mechanism, e.g., guides and bearings with rolling elements, deteriorates the positioning accuracy [3]-[6].

The notable point of the rolling friction is the position dependent property [3], [6]: in the micro displacement region (so-called "presliding region"), contact points between the rolling elements and the guides deform and slip, and the rolling friction generates nonlinear and dynamic friction force. In the macro displacement region (so-called "rolling region"), on the other hand, the rolling elements effectively roll, and the friction force statically behaves as Coulomb friction. In the micrometer stroke positioning motion, therefore, the rolling friction would mainly behave in the presliding region. Reference [2] has pointed out that the rolling friction would cause a response variation between reversal and inching positioning trials in a sequential positioning motion. However, a mechanism of the variation has not yet been exactly clarified in literature. An analytical examination and an effective compensator design for the variation have been remained as a subject matter to be solved.

In this paper, the mechanism of the response variation in the fast and precise micrometer stroke positioning is analytically examined by using a rolling friction model, while a rolling friction model-based simple and commonly-used feedforward (FF) friction compensation is provided with the aim at improving the positioning accuracy. In the mechanism examination, experimental rolling friction behaviors in the sequential positioning motion is analyzed in detail, and it is clarified that a nonlinear elastic property of the rolling friction causes the response variation. In the friction compensation design, on the other hand, the rolling friction model is adopted as an FF compensator to compensate for the nonlinear elasticity. The analysis and the FF friction compensation are examined by numerical simulations and experiments using a laboratory prototype of linear motor-driven table positioning devices.

## II. Table Positioning System

### A. System Configuration

Fig. 1 shows a schematic configuration of the target table positioning system as a prototype. A table with a flexible load is driven by an AC single magnet core type linear motor (rated output of $1.0$ kW, rated thrust of $150$ N, and rated speed of $2.4$ m/s). The table is guided by two rolling ball guides (linear guides) on a machine stand, and the rolling friction (Coulomb friction force $T_{fc}$ of $16.5$ N) is generated at contact points between rolling elements and the guides with lubricant grease. The machine stand is supported by six leveling bolts on floor. The table position is detected by a linear scale (resolution of $0.1$ $\mu$m) along the guides, and is controlled in a full-closed position control manner by a DSP (sampling time $T_s$ of $500$ $\mu$s) and an AC servo amplifier. A current controller in the servo amplifier controls the motor thrust with its control bandwidth of $750$ Hz.

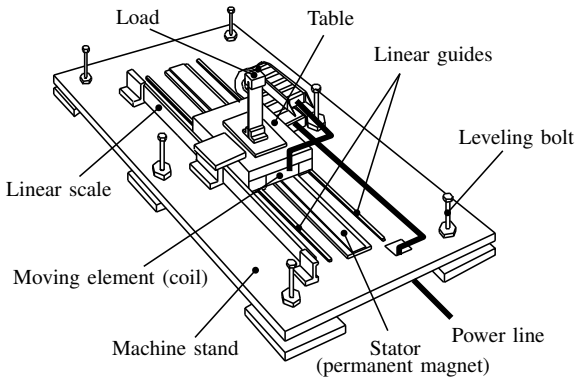


Fig. 1. Schematic configuration of prototype.

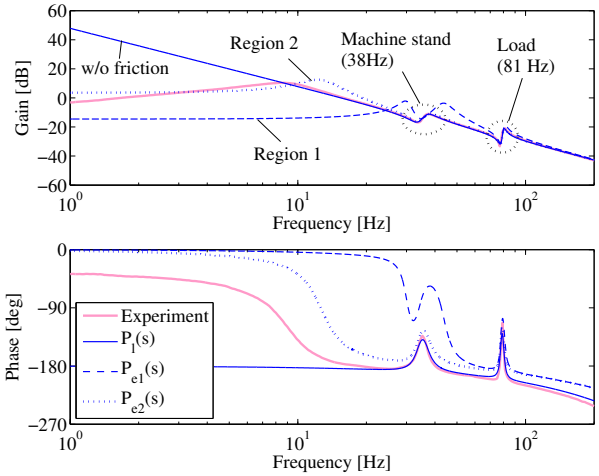


Fig. 2. Bode plots of table position for motor thrust reference.

## B. Frequency Characteristic

Light lines in Fig. 2 show an experimental bode plot of the table position $x_T$ for the motor thrust reference $u_M$ as a control input in a macro displacement region (more than 1 mm). There are two vibration modes at 38 and 81 Hz due to mechanical resonance vibrations of the machine stand with the leveling bolts and the table with the flexible load. In addition to this, the amplitude decreases in the low frequency range less than 10 Hz due to the nonlinear friction generated at the linear guides [5]. A linear plant model $P_l(s)$ is formulated as follows, by considering the two vibration modes:

$$P_l(s) = \frac{x_T(s)}{u_M(s)} = e^{-Ls} K_t \left( \frac{k_{t0}}{s^2} + \sum_{i=1}^{2} \frac{k_{ti}}{s^2 + 2\zeta_{ti}\omega_{ti}s + \omega_{ti}^2} \right) \quad (1)$$

where $L$ is the equivalent dead time, $K_t$ is the motor thrust constant, $\omega_{ti}$ is the natural angular frequency of the $i$-th vibration mode, $\zeta_{ti}$ is the damping coefficient, and $k_{ti}$ is the vibration mode gain, respectively. A bode plot of $P_l(s)$ is depicted by dark solid lines in Fig. 2, which precisely reproduces the experimental frequency characteristic except influence of the friction less than 10 Hz.

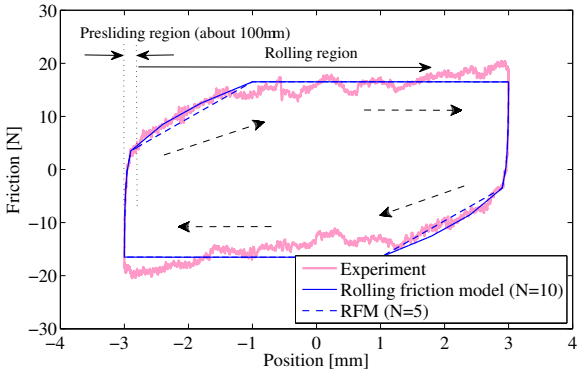


(a) Overview

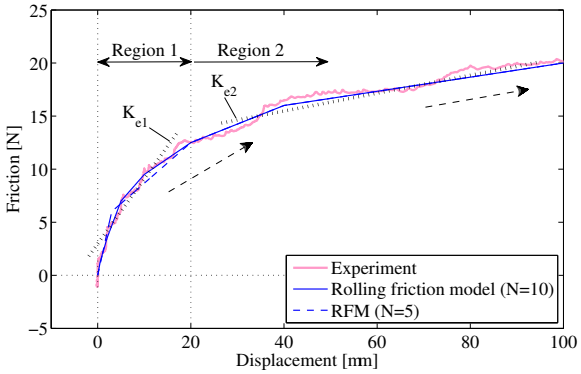


(b) After vel. reversal

Fig. 3. Nonlinear elastic characteristics of rolling friction.

## C. Rolling Friction Characteristic

The rolling friction generates nonlinear elastic friction force with a hysteresis property due to deformation and slips at contact points between rolling elements and rolling ball guides with lubricant grease. The hysteresis curve, in addition, varies depending on position trajectories of past motions ("history dependency" in the following) [5], [6].

Light lines in Fig. 3 show actual rolling friction characteristic of the prototype, where Fig. 3(a) indicates an overview of the hysteresis property and Fig. 3(b) indicates a magnified hysteresis curve just after the velocity reversal. These figures explicitly show that the actual rolling friction can be characterized as a nonlinear elastic component with a hysteresis property, where the presliding region is about 100 $\mu$m. The comprehensive slope of the hysteresis curve varies as shown by "Region 1" and "Region 2" in Fig. 3(b), and the boundary between Region 1 and Region 2 is about 20 $\mu$m. The slope in Region 1 is the steepest in the curve [3]. The comprehensive slope in each region can be approximated from the experimental result as $K_{e1} = 800$ N/m in Region 1 and $K_{e2} = 100$ N/m in Region 2 as indicated by dark dotted lines in Fig. 3(b).

A light line in Fig. 4, on the other hand, depicts an experimental hysteresis characteristic with several internal loops.

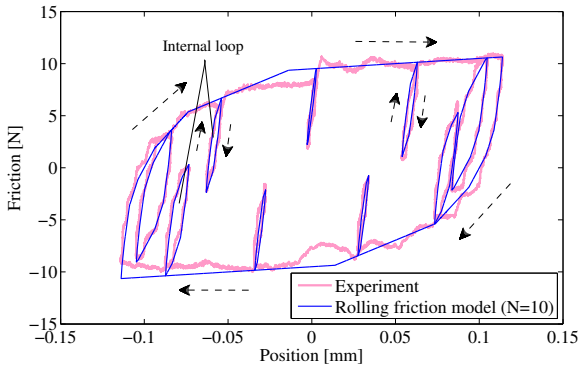


Fig. 4. History dependency of rolling friction.

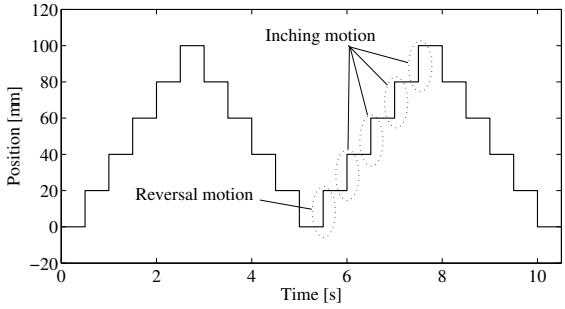


Fig. 5. Waveform of position reference.

From the figure, the hysteresis curve of the rolling friction dynamically varies depending on the position trajectory [5], [6].

### D. Target Positioning Specification

In this study, a table position reference with amplitude of 20 $\mu$m is given, and the table position should settle to the target position with the accuracy of $\pm 2$ $\mu$m by the settling time of 25 ms. In addition, a sequential positioning motion as shown in Fig. 5 that is a combination of reversal and inching motions is performed with the inching interval of 0.5 s, in consideration to a typical positioning motion with the micrometer stroke positioning in industry.

## III. Response Variation in Micrometer Stroke Positioning

### A. 2-Degree-of-Freedom Position Control System

Fig. 6 shows a block diagram of a two-degree-of-freedom (2DoF) table position control system, where $N_{ff}(z)$ and $D_{ff}(z)$ are the FF compensators based on a deadbeat control framework [7] with the linear plant model $P_l(z)$ of eq.(1), $z^{-2}$ is the dead time compensator by Smith method, $C(z)$ is the PID-type FB compensator, $r$ is the target table position (step input), $x_T^*$ is the target table position trajectory reference, and $u_{ff}$ is the FF motor thrust reference, respectively. $N_{ff}(z)$ and $D_{ff}(z)$ are designed so that $x_T^*$ settles to the target position by 20 ms while eliminating vibratory responses in $x_T$. Note that this 2DoF point-to-point positioning control system is equivalent to a continuous position tracking control for $x_T^*$ to achieve the desired positioning performance, where the FB control should suppress the position tracking error by compensating for effects of the rolling friction and/or modeling errors for $P_l(s)$ of eq.(1).

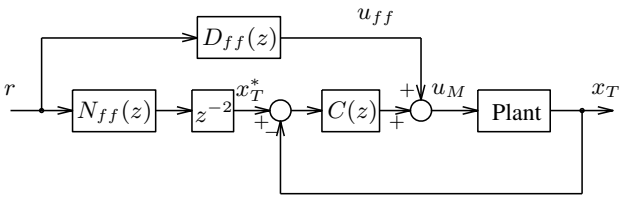


Fig. 6. Block diagram of 2DoF table position control system.

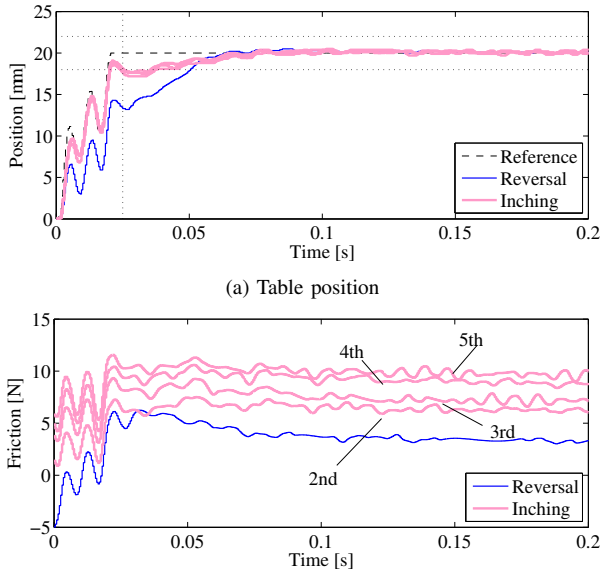


(a) Table position

(b) Estimated friction

Fig. 7. Experimental response waveforms of table position and estimated friction.

### B. Response Variation Between Reversal and Inching Motions

Fig. 7(a) shows experimental response waveforms of the table position $x_T$ for the sequential 20 $\mu$m stroke positioning motion shown in Fig. 5, using the 2DoF control system of Fig. 6. In the figure, five response waveforms when the table moves to the positive direction after the motion direction reversal are indicated. A dark broken line is the target position trajectory reference $x_T^*$, a dark solid line is the response of the first inching motion after the motion direction reversal, and light solid lines are the ones after the second inching motion. It can be explicitly recognized that a remarkable response variation appears between the reversal and the inching motions. In particular, the reversal motion seriously deteriorates the position tracking performance for $x_T^*$ during the transient, and needs 52 ms (the target settling time is 25 ms) to settle within the target settling accuracy of $\pm 2$ $\mu$m indicated by horizontal dotted lines in the figure. As mentioned earlier, the response variation should be compensated by the disturbance

suppression capability of the FB control in the 2DoF control system shown in Fig. 6. However, in general, expanding the servo bandwidth enough is difficult because of a trade-off with stability. Furthermore, since a short stroke positioning motion requires a shorter positioning time comparing to a long stroke one, the variation is easy to appear conspicuously in the micrometer stroke positioning. In order to improve the positioning accuracy, therefore, an FF compensation considering a mechanism of the variation should be one of the effective approaches.

## IV. Rolling Friction Model-Based Analysis of Response Variation

In this section, the response variation in the sequential positioning motion is analyzed while focusing on the rolling friction property and then, the mechanism of the variation is clarified by numerical simulations using a rolling friction model.

### A. Analysis of Response Dispersion Mechanism

In order to examine the mechanism of the response variation between the reversal and the inching motions, response waveforms of friction $\widehat{f}$, which is estimated by a disturbance observer offline, in the sequential positioning motion are indicated in Fig. 7(b). From the figure, the friction force varies in every positioning motion, and the steady force increases with the progress of the feeding motion. A light line in Fig. 8 shows Lissajous waveform of $\widehat{f}$ for $x_T$ indicated in Fig. 7, where vertical dotted lines represent the target positions $(20, 40, 60, 80, 100\ \mu\mathrm{m})$ in each positioning motion. From the figure, comprehensive slopes of the elasticity are quite different between the reversal and the inching motions as depicted by dark dotted lines, and each slope is almost equivalent to the one of the nonlinear elastic property of the rolling friction (Region 1 is 800 N/mm and Region 2 is 100 N/mm) shown in Fig. 3(b). Namely, it is considered that the reversal and the inching motions are performed in Region 1 and Region 2 of the rolling friction.

The equivalent plant model $P_{ei}(s)(i = 1, 2)$ in the micro displacement region is mathematically expressed as follows, using an elastic coefficient $K_{ei}$ of the rolling friction and the linear plant model $P_l(s)(= P_l'(s)e^{-Ls})$ in the macro displacement region defined by eq.(1):

$$P_{ei}(s) = \frac{x_T(s)}{u_M(s)} = \frac{P_l'(s)}{1 + K_{ei}P_l'(s)}e^{-Ls}. \tag{2}$$

Fig. 9 shows a block diagram of $P_{ei}(s)$, while its frequency characteristics in Region 1 and Region 2 are indicated by dark broken lines and dark dotted lines in Fig. 2. From Fig. 2, the plant system can be regarded as an elastic component in the micrometer stroke positioning, and the behavior varies depending on the displacement region of the rolling friction. In the following sections, in order to verify the above mentioned examination, the rolling friction in the mechanism is mathematically modeled by a rheology-based rolling friction model [5], and reproductivity of the response variation is comparatively evaluated between the experiment and a numerical simulation.

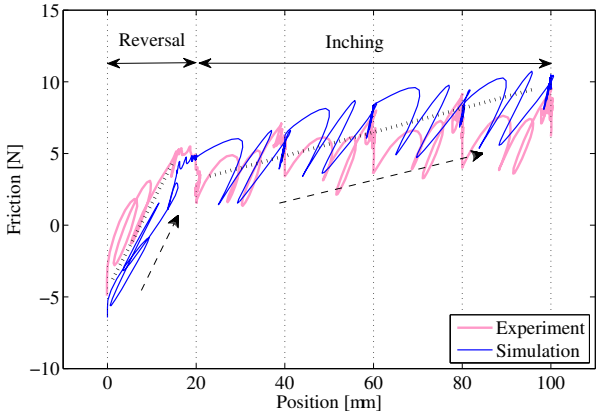


Fig. 8. Lissajous waveforms of rolling friction for table position in sequential positioning motion.

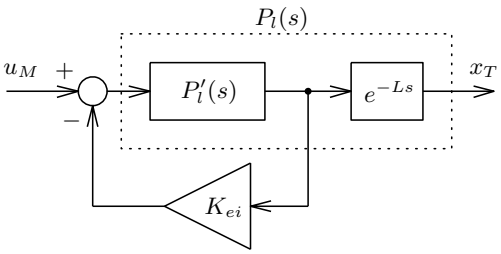


Fig. 9. Equivalent plant model $P_{ei}(s)$ in micro displacement region.

### B. Rolling Friction Model

The rolling friction model [5] is a multiple-structure friction model such as an elastoplastic model [8] and Generalized Maxwell Slip model [6] that can well express friction phenomena at contact points of friction surfaces due to asperity. Fig. 10 shows an elementary rheology model and its force characteristic for displacement, while Fig. 11 shows the rolling friction model which consists of $N$ elementary models in parallel. The rolling friction model can be mathematically formulated as follows:

$$x_i = \begin{cases} x + x_{ri} & (|x_i| < X_{mi}) : \text{ stick} \\ \mathrm{sgn}(\frac{dx}{dt})X_{mi} & (|x_i| = X_{mi}) : \text{ slip} \end{cases} \tag{3}$$

$$f_i = K_i x_i + D_i \frac{dx_i}{dt} \tag{4}$$

$$F_{mi} = K_i X_{mi} \tag{5}$$

$$-X_{mi} \le x_i \le X_{mi} \tag{6}$$

$$-F_{mi} \le f_i \le F_{mi} \tag{7}$$

$$f_{rolling} = \sum_{i=1}^{N} f_i \tag{8}$$

where $x$ is the displacement input corresponding to the table position $x_T$, $x_i$ is the element displacement, $x_{ri}$ is the element displacement at velocity reversal, $f_i$ is the element force, $X_{mi}$

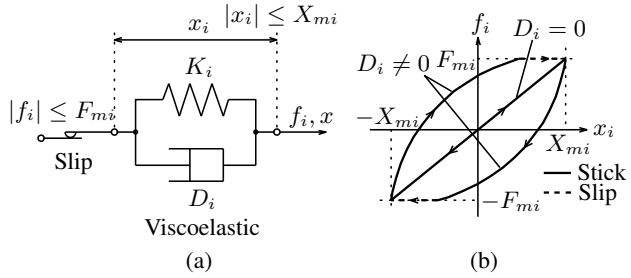


Fig. 10. Elementary model based on rheology.

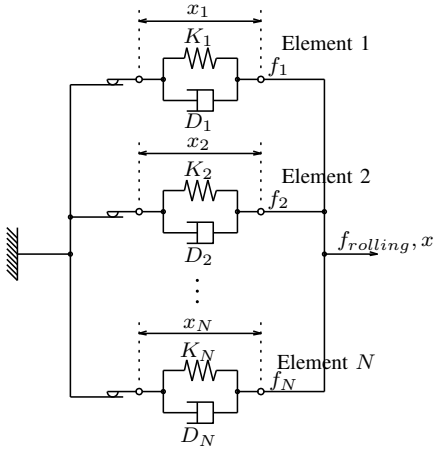


Fig. 11. Rolling friction model with $N$ elementary models.

is the maximum element displacement, $F_{mi}$ is the maximum element force, $K_i$ is the element elastic coefficient, $D_i$ is the element viscous coefficient, sgn$(\cdot)$ is the sign function, and $f_{rolling}$ is the rolling friction force, respectively. From eqs.(3)-(7), the elementary model generates viscoelastic friction force in the stick region and the static force with the limit stress of $\pm F_{mi}$ in the slip region. By introducing the multiple-structure concept with the elementary model, the rolling friction model can represent the complicated hysteresis curve as well as the history dependency of the rolling friction [6], [8]. The parameters of the rolling friction model, i.e., $K_i$, $D_i$, and $F_{mi}$, are identified by using Back Propagation algorithm, while $N$ is decided so that an evaluation function for a square error between the experimental data and the model output is minimized [5]. Dark solid lines indicated in Figs. 3 and 4 show the hysteresis characteristics of the rolling friction model with $N = 10$. The rolling friction model well reproduces the actual rolling friction characteristics indicated by the light lines.

### C. Simulation of Sequential Micrometer Stroke Motion

Fig. 12 shows simulation response waveforms of the table position $x_T$ and the rolling friction $f_{rolling}$ for the same sequential positioning motion as of the experiment shown in Fig. 7. Note that the plant model in the numerical simulation is composed of $P_l(s)$ of eq.(1) and the rolling friction model of eqs.(3)-(8), i.e., the rolling friction model is considered as $K_{ei}$ in Fig. 9. Actually, although a stiction force and stribeck

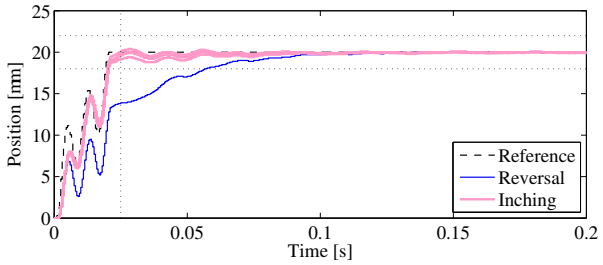


(a) Table position

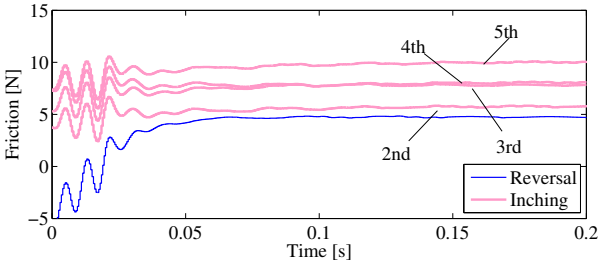


(b) Rolling friction

Fig. 12. Simulation response waveforms of table position and rolling friction.

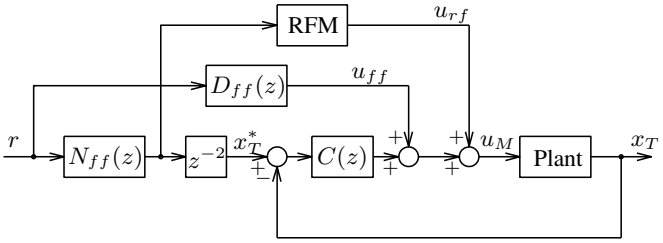


Fig. 13. Block diagram of 2DoF table position control system with RFM-based FF friction compensation.

effect model and a viscous friction model are simultaneously considered with the rolling friction model, those effects are quite small in the micrometer stroke motion. The simulation result expresses the response variation between the reversal and the inching motions as well as the friction variation in the steady state in each positioning motion, which well reproduce the experimental result shown in Fig. 7. A dark solid line indicated in Fig. 8 shows Lissajous waveform of $f_{rolling}$ for $x_T$ in the simulation. From the figure, the rolling friction generates different elastic force between the reversal and the inching motions as the experimental result indicated by the light line.

From the series of the simulation analyses, it is clarified that the nonlinear elastic property of the rolling friction, i.e., the difference in Region 1 and Region 2, causes the response variation in the sequential micrometer stroke positioning.

## V. Model-Based FF Friction Compensation and Experimental Evaluation

### A. Model-Based FF Friction Compensation

Since the rolling friction model designed in Section IV-A can reproduce the nonlinear elastic property of the rolling

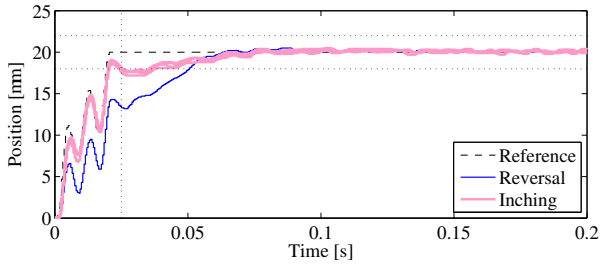


(a) w/o RFM-based FF Comp.

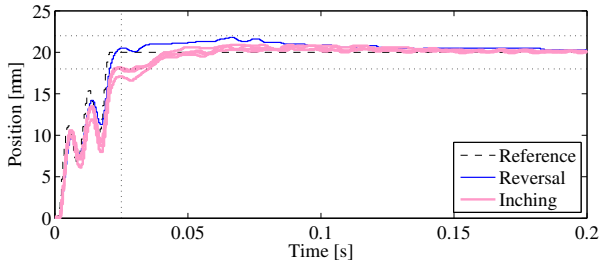


(b) w/ RFM-based FF Comp.

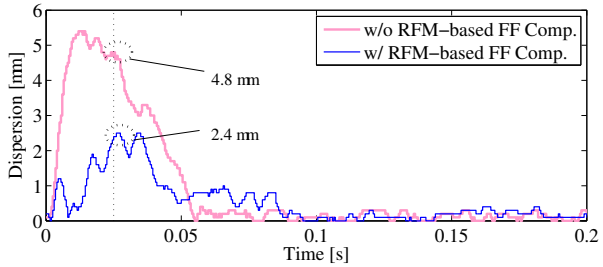


(c) Dispersion

Fig. 14. Experimental response waveforms of table position and its dispersion without and with RFM-based FF friction compensation.

friction and the response vatiation, a rolling friction model-based FF friction compensation is simply adopted in this study. Fig. 13 shows a block diagram of the 2DoF position control system with the FF friction compensation, where RFM is the simplified rolling friction model as an FF compensator and $u_{rf}$ is the FF friction compensation force. The number $N$ of RFM is determined as $N = 5$ in consideration to the reproductivity for the nonlinear elastic property, especially paying attention to the presliding region. Dark broken lines in Fig. 3 show RFM with $N = 5$, which expresses the comprehensive slopes of the actual rolling friction in Region 1 and Region 2. In the RFM-based FF friction compensation, the target position trajectory reference $x_T^*$ is input to RFM to cancel the actual rolling friction force by $u_{rf}$ without a compensation delay.

### *B. Experiment of Micrometer Stroke Motion*

Effectiveness of the RFM-based FF friction compensation is verified by an experiment of 20 $\mu$m stroke sequential positioning motion. In the experiment, in order to evaluate the dispersion in the table position $x_T$, $3\sigma$ ($\sigma$ is the standard deviation) of $x_T$ for sequential five feeding positioning trials to the positive direction is calculated. Fig. 14 shows comparative response waveforms of $x_T$ and its dispersion in the cases without and with the RFM-based FF compensation. In the case with the RFM-based FF compensation shown in Fig. 14(b), the reversal motion indicated by a dark solid line follows the target trajectory reference $x_T^*$ during the transient better than the case without the RFM-based FF compensation shown in Fig. 14(a). As a result, the table position settles to the target position within the accuracy of $\pm 2$ $\mu$m until the target settling time of 25 ms, and the response dispersion after 25 ms is reduced to 2.4 $\mu$m from 4.8 $\mu$m. The inching motions indicated by light lines in Fig. 14(b), however, cannot satisfy the target control specifications because of the dispersion. From the experimental evaluation, although the designed simple and commonly-used FF friction compensation is effective for suppressing the response variation between the reversal and inching motions, the response dispersion caused by unknown phenomena still remains and deteriorates the settling accuracy. Analyses and effective compensation design for the dispersion will be examined as one of the future challenges.

## VI. Conclusion

In this paper, an analytical examination of a response variation have been presented for the fast and precise micrometer stroke positioning of linear motor-driven table positioning devices. In the mechanism examination, it has been clarified by numerical simulations using a rolling friction model that a nonlinear elastic property of rolling friction causes the variation between reversal and inching positioning motions. On the other hand, a rolling friction model-based simple FF friction compensation has been applied to improve the positioning accuracy. As a result, although the response dispersion could be reduced to 50 % of the case without the FF friction compensation, the target control specifications have not yet been satisfied due to the remained response dispersion. The reason of the variation and an effective compensation design will be considered as a future work.

## References

[1] D. Matsuka, S. Fukushima, and M. Iwasaki, "Compensation for Torque Fluctuation Caused by Temperature Change in Fast and Precise Positioning of Galvanometer Scanners," in *Proc. 2015 IEEE Int. Conf. Mechatron.*, Nagoya, Japan, 2015, pp. 638–643.

[2] W. Maebashi, K. Ito, and M. Iwasaki, "Robust Fast and Precise Positioning with Feedfoward Disturbance Compensation," in *Proc. 37th Int. Conf. IEEE Ind. Electron. Society*, Melbourne, Australia, 2011, pp. 3418–3423.

[3] S. Futami, A. Furutani, and S. Yoshida, "Nanometer positioning and its micro-dynamics," *Nanotechnology*, vol. 1, no. 1, pp. 31–37, 1990.

[4] H. Asaumi and H. Fujimoto, "Proposal on nonlinear friction compensation based on variable natural length spring model," in *Proc. SICE Annu. Conf.*, Tokyo, Japan, 2008, pp. 2393–2398.

[5] Y. Maeda and M. Iwasaki, "Initial Friction Compensation Using Rheology-Based Rolling Friction Model in Fast and Precise Positioning," *IEEE Trans. Ind. Electron.*, vol. 60, no. 9, pp. 3865–3876, 2013.

[6] M. Boegli, T. D. Laet, J. D. Schutter, and J. Swevers, "A Smoothed GMS Friction Model Suited for Gradient-Based Friction State and Parameter Estimation," *IEEE Trans. Mechatron.*, vol. 19, no. 5, pp. 1593–1602, 2014.

[7] Y. Maeda and M. Iwasaki, "Improvement of Adaptive Property by Adaptive Deadbeat Feedforward Compensation Without Convex Optimization," *IEEE Trans. Ind. Electron.*, vol. 62, no. 1, pp. 466–474, 2015.

[8] G. Ferretti, G. Magnani, and P. Rocco, "Single and multistate integral friction models," *IEEE Trans. Automatic Control*, vol. 49, no. 12, pp. 2292-2297, 2004.